Primary Ovarian Insufficiency and Azoospermia in Carriers of a Homozygous *PSMC3IP* Stop Gain Mutation

Abdulmoein Eid Al-Agha,[1] Ihab Abdulhamed Ahmed,[1] Esther Nuebel,[2] Mika Moriwaki,[3] Barry Moore,[4] Katherine A. Peacock,[3] Tim Mosbruger,[5] Deborah W. Neklason,[6] Lynn B. Jorde,[4] Mark Yandell,[4] and Corrine K. Welt[3]

[1]Pediatric Department, King Abdulaziz University Hospital, Jeddah 21589, Saudi Arabia; [2]Howard Hughes Medical Institute and Department of Biochemistry, University of Utah, Salt Lake City, Utah 84112; [3]Division of Endocrinology, Metabolism and Diabetes, University of Utah, Salt Lake City, Utah 84112; [4]UStar Center for Genetic Discovery, Department of Human Genetics, University of Utah, Salt Lake City, Utah 84112; [5]Bioinformatics, Huntsman Cancer Institute, University of Utah, Salt Lake City, Utah 84112; and [6]Division of Genetic Epidemiology, Department of Internal Medicine, University of Utah, Salt Lake City, Utah 84112

Context: The etiology of primary ovarian insufficiency (POI) remains unknown in most cases.

Objective: We sought to identify the genes causing POI.

Design: The study was a familial genetic study.

Setting: The study was performed at two academic institutions.

Patients: We identified a consanguineous Yemeni family in which four daughters had POI. A brother had azoospermia.

Intervention: DNA was subjected to whole genome sequencing. Shared regions of homozygosity were identified using Truploidy and prioritized using the Variant Annotation, Analysis, and Search Tool with control data from 387 healthy subjects. Imaging and quantification of protein localization and mitochondrial function were examined in cell lines.

Main Outcome: Homozygous recessive gene variants shared by the four sisters.

Results: The sisters shared a homozygous stop gain mutation in exon 6 of *PSMC3IP* (c.489 C>G, p.Tyr163Ter) and a missense variant in exon 1 of *CLPP* (c.100C>T, p.Pro34Ser). The affected brother also carried the homozygous *PSMC3IP* mutation. Functional studies demonstrated mitochondrial fragmentation in cells infected with the *CLPP* mutation. However, no abnormality was found in mitochondrial targeting or respiration.

Conclusions: The *PSMC3IP* mutation provides additional evidence that mutations in meiotic homologous recombination and DNA repair genes result in distinct female and male reproductive phenotypes, including delayed puberty and primary amenorrhea caused by POI (XX gonadal dysgenesis) in females but isolated azoospermia with normal pubertal development in males. The findings also suggest that the N-terminal missense mutation in *CLPP* does not cause substantial mitochondrial dysfunction or contribute to ovarian insufficiency in an oligogenic manner. (*J Clin Endocrinol Metab* 103: 555–563, 2018)

Primary ovarian insufficiency (POI) is characterized by early ovarian follicle depletion, resulting in low estradiol and elevated follicle-stimulating hormone (FSH) levels in women aged <40 years (1). The known causes of nonsyndromic POI are expanding, yet the etiology in most clinical cases remains unknown.

Abbreviations: FSH, follicle-stimulating hormone; GFP, green fluorescent protein; LOH, loss of heterozygosity; mGFP, monomeric green fluorescent protein; Mut, mutant; OCR, oxygen consumption rate; POI, primary ovarian insufficiency; SDS, sodium dodecyl sulfate; TBST, Tris-buffered saline plus Tween 20; VAAST, Variant Annotation, Analysis, and Search Tool; WT, wild-type.

POI has a strong genetic component (2, 3). A close relationship has been found between the age at menopause in mothers and daughters (2). Twin studies have estimated heritability at 53% to 71% (3, 4). Therefore, many groups have taken a genetic approach to uncover the missing etiologies in women with POI. A remarkable number of new genes have been discovered in the past 2 years, facilitated by whole exome sequencing in consanguineous families (5–10). Many of the mutations in consanguineous families cause primary amenorrhea associated with POI (XX gonadal dysgenesis), suggesting that they have a very deleterious effect on the underlying germ cell pool. The mutations identified in consanguineous families in the absence of other syndromic features have been found in genes important for meiosis, homologous recombination, and DNA damage and repair (5–7, 9, 10). Other syndromic disorders have also been associated with primary amenorrhea and POI in consanguineous families, including vanishing white matter disease with POI (11) and Perrault syndrome with associated deafness (12–14).

In the absence of syndromic features, few examples are available of genes affecting both male and female germ cells. Some gene mutations cause failure of gonadal development, including both germ cells and steroidogenesis in males and females (15). Others affect germ cells in males and females but steroidogenesis only in females (5, 9, 16, 17). We report a consanguineous family from Yemen in which four daughters had a diagnosis of delayed puberty, primary amenorrhea, and ovarian insufficiency with no associated syndromic features. The oldest brother in the family was found to have azoospermia and normal pubertal development. The subjects shared a homozygous stop gain mutation in *PSMC3IP*, a gene that affects male and female germ cell meiosis, homologous pairing, and double strand break repair. The mutation highlights the distinct differences in germ cell development, steroidogenesis, and fertility between men and women.

Materials and Methods

Clinical case report

The parents of the affected girls are first cousins from Yemen. The proband (age 27 years) was identified in a pediatric practice when she presented with the absence of thelarche, primary amenorrhea, and POI (Fig. 1). She had streak gonads and an elevated FSH level. Her karyotype was normal. Three sisters (aged 24, 17, and 14 years) and the paternal aunt also had absence of thelarche, primary amenorrhea, and POI, with elevated FSH levels. The youngest daughter, aged 6 years at the time of our study, had not yet reached puberty. The oldest boy in the family (aged 29 years) had undergone normal pubertal development, had been married for 8 years without a pregnancy, and had a diagnosis of azoospermia. The other boys had
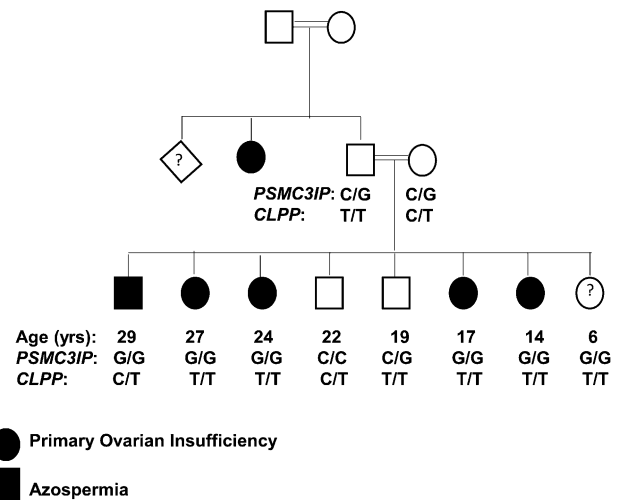

Figure 1. Pedigree of a Yemeni family with homozygous mutations in *PSMC3IP* and *CLPP*. The women affected with POI are indicated by filled circles. Ages and genotypes confirmed with Sanger sequencing are indicated for *PSMC3IP* and *CLPP*. *CLPP* genotype c.100C>T results in p.Pro34Ser. *PSMC3IP* genotype c.489C>G results in a stop gain mutation, p.Tyr163Ter.

normal pubertal development and were not married. The family had no other medical problems and no hearing impairment.

Replication subjects with POI

DNA from 96 subjects with nonsyndromic POI diagnosed at varying ages was studied for replication. These patients had a normal karyotype and *FMR1* repeat lengths and negative adrenal cortical antibody testing.

Control subjects

The control subjects consisted of 96 unrelated, unaffected, whole genome–sequenced controls of European ancestry recruited for health in old age through the Utah Genome Project. In addition, whole genome sequences from 291 CEU (Utah residents), FIN (Finnish in Finland), and GBR (British in England and Scotland) samples from the 1000 Genomes Project were used as unaffected controls (18). The Saudi Human Genome Program was also queried for population-specific variant frequency.

The Partners Human Research Committee and the institutional review board of the University of Utah approved the study for all POI subjects. All subjects gave written informed consent or assent with parental consent.

Genetic studies

DNA was extracted from whole blood using the QIAmp DNA Blood Maxi Kit (Qiagen, Valencia, CA). Based on the possibility that the disorder was X-linked, given the POI in the paternal aunt, a high-resolution X chromosome oligonucleotide microarray was performed on the proband (Pittsburgh Cytogenetics Laboratories, Pittsburgh, PA). In addition, whole genome libraries were prepared using the KAPA Hyper prep kit and sequenced on the Illumina X Ten sequencing platform to a depth of >55X by NantOmics (Culver City, CA) for family members and controls. The 96 unrelated women with sporadic POI underwent whole exome sequencing using the Illumina HiSEquation 2000 by the High-Throughput Genomics and

Bioinformatics Analysis Core (Huntsman Cancer Center, University of Utah, Salt Lake City, UT). DNA libraries were prepared using the Agilent SureSelectXT Human All Exon + UTR, version 5 (Agilent Technologies, Santa Clara, CA).

Variants from all case and control samples were called according to the UGP 1.3.0 variant calling pipeline (available at: http://weatherby.genetics.utah.edu/UGP/wiki/index.php/UGP_Variant_Pipeline_1.3.0). In brief, reads were aligned to GRCh37, decoy sequence, and phiX using bwa (version 0.7.10). Duplicates were marked using samblaster (version 0.1.22). The resulting bam files were polished using GATK (version 3.3-0) IndelRealigner and BaseRecalibrator. Variants were called using GATK HaplotypeCaller, limiting to regions targeted in the Agilent SureSelectXT Clinical Research Exome kit (Agilent Technologies). Genotyping was performed using GATK GenotypeGVCFs on the variant calls plus the controls. Variant calls were recalibrated with GATK VariantRecalibrator.

Genomic analysis

Data were analyzed using Opal 4.15 (Fabric Genomics, Inc., Oakland, CA) in a four-person Variant Annotation, Analysis, and Search Tool (VAAST) cohort analysis that included the affected sisters (available at: https://app.omicia.com/). VAAST does not consider the genetic relatedness between individuals but was the preferred choice for our family because pedigree VAAST does not model consanguinity (19, 20). Although the P values on a cohort analysis with related individuals would not be valid and thus not considered, the scoring and filtering functions provided a valuable form of analysis for an otherwise challenging data set. Candidate variants were filtered with Opal (Fabric Genomics, Inc.) to exclude noncoding and synonymous variants and variants with a reported allele frequency of >1% in three publicly available databases: the 1000 Genomes Project (18); the ExAC database, which includes whole exome sequencing from > 60,000 subjects without severe pediatric disease (21); and the Exome Variant Server, which includes whole exome sequencing from subjects with cardiovascular or cerebrovascular disease, hypertension, or hyperlipidemia and unaffected controls (22). In addition, nonpathogenic variants found in other families (n = 2) with a known mutation in a different gene and variants in genes known to demonstrate an excess of false-positive results were filtered. Variants were prioritized using the Omicia score, which ranks variants according to expected protein effects using SIFT (available at: http://sift.jcvi.org/), Mutation Taster (available at: http://www.mutationtaster.org/), PolyPhen (available at: http://genetics.bwh.harvard.edu/pph2), and PhyloP (23–25). The Phenotype Driven Variant Ontological Reranking tool (26) was used to rerank the prioritized genes using premature ovarian failure and POI as the human phenotype ontology seed terms (27).

The sequenced members of the family were further searched for loss of heterozygosity (LOH) regions with a software tool called "Truploidy," developed by the Utah Genome Project. Truploidy uses population variant frequency data from resources such as ExAC (21) to derive an expected rate of heterozygosity for sliding windows across the genome. This information is then combined in a Bayesian model to derive a posterior probability for three situations: the region in the window (1) is "normal" (*e.g.,* fits the population expectation of heterozygosity) (2); exhibits "LOH"; or (3) is "deleted."

Plasmid preparation

Human *CLPP* cDNA in a lentiviral targeting vector with a monomeric green fluorescent protein (mGFP) tag (pLenti-C-mGFP; no. PS100071; Origene, Rockville, MD) was purchased. The point mutation c.100C>T was introduced using the oligonucleotides 5′-CGCAGCGGCCGTCGCAGCGGACA-3′ and 5′-TGTCCGCTGCGACGGCCGCTGCG-3′ in the Quik-Change II XL Site-Directed Mutagenesis Kit (Agilent Technologies). Lentiviral plasmids were propagated in Stbl3 chemically competent *Escherichia coli* (Life Technologies, Carlsbad, CA) under chloramphenicol selection and verified by DNA sequencing.

Lentiviral transduction

All lentiviral transductions were performed with pseudotyped third-generation lentiviral supernatants generated by cotransfection of HEK293T cells with vectors pMD2.G (Addgene no. 12259; Addgene, Cambridge, MA), pMDLG/pRRE (Addgene no. 12251), pRSV-Rev (Addgene no. 12253), and pLenti-C-mGFP harboring *CLPP* using Lipofectamine 2000 (Invitrogen).

PA-1 cell model

PA-1 cells (American Type Culture Collection, Manassas, VA) were used for the experiments. The expression pattern in these cells is similar to that of embryonic stem cells and has been validated previously (28).

PA-1 cells were grown in supplemented Dulbecco's modified Eagle medium. Cells were plated at 3.5×10^4 cells per well on a six-well plate and infected with lentivirus containing *CLPP* wild-type (WT) or *CLPP* mutant (Mut) plasmid after reaching 80% confluence. Stable cell lines were generated by selection for GFP expression in an Avalon Cell Sorter (Propel Laboratories, Fort Collins, CO) at the Flow Cytometry Core of the University of Utah.

Cell imaging

Cells were plated in six-well imaging chambers at a density of 1×10^6 and grown to 35% confluence. The cells were then treated with 25 nM Mitotracker Red CMXRos (Life Technologies) and 16.2 μM Hoechst 33342 (Thermo Fisher Scientific) and incubated for 10 minutes, followed by a 10-minute wash with media without dyes before imaging, as described previously (29). The cells were imaged on the Axio Observer Z1 imaging system (Carl Zeiss) equipped with 10×, 40×, and 100× objectives (oil immersion). Digital fluorescence and differential interference contrast images were acquired using a monochrome digital camera (AxioCam MRm; Carl Zeiss). The final images were adjusted and assembled using Adobe Photoshop CS5. Brightness and contrast were adjusted using only the linear operation on the entire image.

Mitochondria isolation

The mitochondrial fraction of PA-1 cells was isolated using a Mitochondria Isolation Kit for Cultured Cells (Thermo Fisher Scientific, Rockford, IL). Isolated mitochondria were lysed with radioimmunoprecipitation assay buffer (150 mM sodium chloride, 1% NP-40, 0.5% sodium deoxycholate, 0.1% sodium dodecyl sulfate (SDS), 50 mM Tris; pH 8.0) containing 1% protease and phosphatase inhibitor cocktail (Thermo Fisher Scientific) for 30 minutes at 4°C. Lysates were centrifuged at 12,000 rpm for 20 minutes at 4°C to isolate soluble

mitochondrial proteins from pellets. The Bio-Rad DC protein assay (Hercules, CA) was used to quantify the mitochondrial protein concentrations.

Western blot

After boiling in Laemmli buffer (Bio-Rad) for 5 minutes, 16 µg of protein from each lysate was separated in 20% SDS-polyacrylamide gel electrophoresis gel for 5 hours at 125 V in Tris-glycine buffer (25 mM Tris-HCl, 192 mM glycine, 3.5 mM SDS; pH 8.3), and transferred to nitrocellulose membranes at 30 V overnight in transfer buffer (25 mM Tris base, 190 mM glycine, 1.7 mM SDS, 20% ethanol). Membranes were blocked in 5% nonfat dry milk in Tris-buffered saline plus Tween 20 (TBST; 20 mM Tris base, 137 mM NaCl, 0.05% Tween 20; pH 7.6) for 1 hour at room temperature and incubated with primary antibodies diluted in 5% nonfat dry milk in TBST overnight at 4°C. The experiment was repeated twice for confirmation using 4 to 16 µg protein from each lysate separated on a 7.5% or 20% SDS-polyacrylamide gel electrophoresis gel for 70 to 110 minutes at 100 to 150 V. The primary antibodies and dilutions used were as follows: mouse anti-mGFP 1:500 (Origene) and rabbit anti-heat shock protein (HSP)60 1:10,000 (Abcam, Cambridge, MA). Membranes were washed with TBST, incubated with horseradish peroxidase–conjugated secondary antibodies (Thermo Fisher Scientific) in 2% nonfat dry milk in TBST for 1 hour at room temperature, and washed again with TBST. Band density on X-ray film was quantified using a GelDoc-It Imager and VisionWorks LS software (UVP, Upland, CA) and normalized according to HSP60 content.

Metabolic profiling

p-Lenti-CLPP-mGFP WT- and Mut-infected PA-1 cells were seeded at 6×10^4 cells per well in a Seahorse XF-96 cell culture microplate (Agilent Technologies) and grown at 37°C in a humidified 5% carbon dioxide incubator for 2 hours. The cellular oxygen consumption rate (OCR) was measured using a Seahorse XF^{e}96 Analyzer (Agilent Technologies) at baseline and after oligomycin, carbonyl cyanide P-trifluoromethoxyphenylhydrazone, and rotenone/antimycin A injections at the Metabolic Phenotyping Core at the University of Utah. The data were analyzed using Wave 2.3 software (Agilent Technologies). After the assay, the cells were washed with ice-cold phosphate-buffered saline, lysed in 20 µL/well of radioimmunoprecipitation assay buffer for 30 minutes at 4°C, and total protein was measured using the DC protein assay (Bio-Rad). The experiment was repeated three times.

Results

A high-resolution X chromosome oligonucleotide microarray was performed on the proband. No alterations in DNA copy number >5 kb were detected, and no clinically relevant X chromosome copy number variants were identified.

Truploidy identified regions with LOH in the family consistent with consanguinity. Truploidy output demonstrated minimal regions of intersection of LOH for the proband and affected sisters using a window size of 1 megabase (Bonferroni $P < 0.05$; Fig. 2).

Analysis using the VAAST algorithm identified nine homozygous recessive gene variants shared by the four affected sisters (Table 1). Only five of the nine homozygous recessive variants were found in regions of homozygosity (chromosomes 17 and 19). Two homozygous
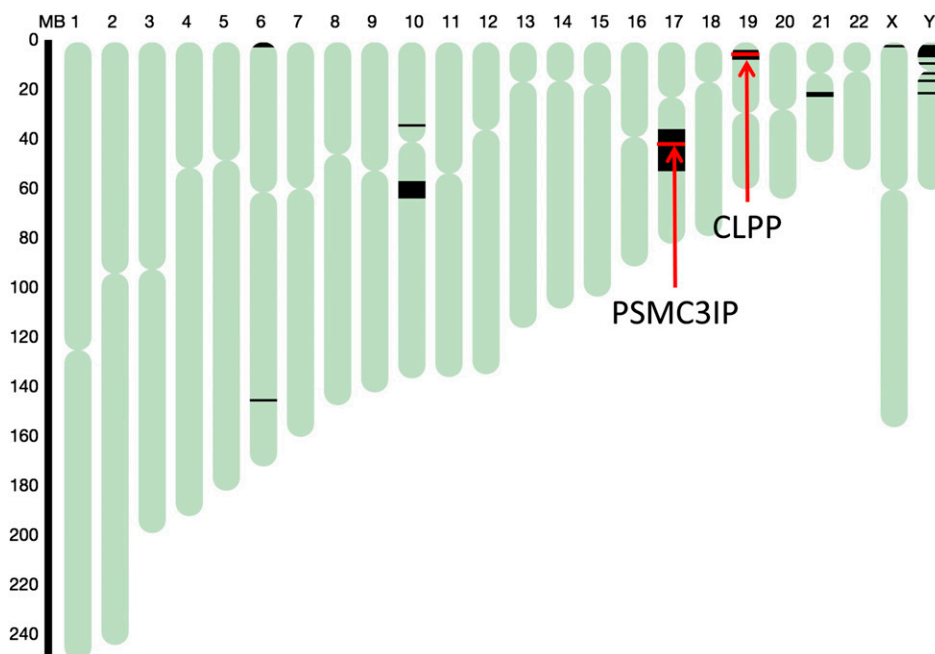

Figure 2. Minimal regions of intersection of LOH for all four probands using a window size of 1 megabase were identified on chromosomes 6, 10, 17, 19, 21, and X (black bars), as determined using Truploidy ($P < 0.05$). Candidate gene locations (red) with variants shared by four affected sisters and found in LOH regions are indicated.

Table 1.   Candidate Coding Gene Variants Shared by Four Sisters With POI Determined Using VAAST Analysis

Gene Symbol	Chromosome	Starting Base Pair	rsID	Base Pair Change	Protein Change	Consequence	1000 Genomes/ ExAC Frequency[a]	Omicia Variant Score[b]	VAAST Rank[c]	VAAST Gene Score[d]	VAAST Variant Score[e]	VAAST P Value[f]
PSMC3IP	17	40725377		c.489C>G	p.Tyr163Ter	STOP	NA/NA	0.786	1	113.902	113.9	1.00E-06
AGAP3	7	150783917	rs775200524	c.89T>G	p.Leu30Arg	MISSENSE	NA/NA	0.074	3	106.948	106.95	1.00E-06
EFCAB13	17	45455258	rs200149627	c.1499C>T	p.Thr500Ile	MISSENSE	NA/0.00001	0.167	18	103.183	103.18	1.00E-06
CLPP	19	6361685	rs776759641	c.100C>T	p.Pro34Ser	MISSENSE	NA/0.00035	0.059	22	102.846	102.85	1.00E-06
TAF4	20	60640461	rs113875178	c.406T>G	p.Ser136Ala	MISSENSE	NA/NA	0.053	33	99.8928	99.89	1.00E-06
UBXN6	19	4446621	rs141014666	c.796G>A	p.Val266Met	MISSENSE	0.0004/0.0023	0.325	53	91.3331	91.33	1.00E-04
FDXR	17	72859001	rs35769464	c.1543A>G	p.Thr515Ala	MISSENSE	0.0022/0.0048	0.07	90	76.9754	76.98	1.00E-04
FOXD4L5	9	70177212		c.772T>C	p.Cys258Arg	MISSENSE	NA/NA	0.043	147	62.1436	62.14	1.00E-04
GTF2IRD2B	7	74542147	rs201207883	c.631G>A	p.Gly211Ser	MISSENSE	NA/NA	0.202	214	49.2687	49.27	1.00E-04

Abbreviations: NA, not available (the variant was not identified in these databases); rsID, reference SNP (single nucleotide polymorphism) cluster identification.

[a]Minor allele frequency in 1000 Genomes (18) or the ExAC Database (21).

[b]The Omicia Variant Score is a proprietary score that assesses whether a variant is likely to be deleterious according to SIFT, PolyPhen, MutationTaster, and PhyloP variant scoring algorithms; scores >0.5 are likely to be damaging base pair changes, with greater confidence for values closer to 1.

[c]The VAAST rank is assigned using the VAAST Gene and Variant scores and the P value.

[d]VAAST Gene Score is the sum of the variant scores for every variant in the gene.

[e]The VAAST Variant Score scores each individual variant in a gene based on the nature of the amino acid change induced and the relative enrichment of the frequency in cases vs controls.

[f]The probability of observing the gene score by random chance.

variants were located in previously identified genes causing POI, *PSMC3IP* (chr17q21.2) and *CLPP* (chr19p13.3; Fig. 2) (12–14, 30).

The Phenotype Driven Variant Ontological Reranking tool, which ranks variants based on a phenotype and gene ontology algorithm, prioritized both the stop gain mutation (c.489 C>G, p.Tyr163Ter) in exon 6 of *PSMC3IP* and the missense variant (c.100C>T, p.Pro34Ser) in exon 1 of *CLPP* as the top two candidates (26). The *PSMC3IP* variant (c.489 C>G) was not identified; however, 4 homozygous and 93 heterozygous *CLPP* variants (c.100C>T) were found in 2369 Saudi exomes. No variants were found in *PSMC3IP* in the replication cohort of 96 women with sporadic POI. One subject carried a heterozygous variant in *CLPP* (c.343A>T, p.Ile115Phe).

Previous studies demonstrated a reduced ovarian size and absence of germ cells in the mouse *PSMC3IP* knockout model (31). However, the missense variant in *CLPP* has not been previously described, and additional functional analyses were performed.

The *CLPP* missense mutation was located in the N-terminal extension of the protein, which is a targeting peptide that directs CLPP into the mitochondria (32). We, therefore, hypothesized that the missense mutation would result in failure to enter the mitochondria. Fluorescence microscopy of PA-1 cells infected with pLenti-CLPP-mGFP WT and Mut demonstrated colocalization of both CLPP WT and Mut in the mitochondria (Fig. 3). A subset of CLPP Mut-infected cells with apparent fragmentation of the mitochondria was found (Fig. 3C, 3D, 3G, 3H, 3K, and 3L). We could confirm the mitochondrial presence of CLPP WT and Mut protein in the mitochondrial fraction with Western blotting (Fig. 4). No

difference was found in the quantity of CLPP-GFP WT or Mut (1.09 ± 0.61 vs 0.93 ± 0.40 CLPP-GFP/HSP60). We could also exclude the possibility of a delay or lack of processing of the precursor into the mature protein, because we did not detect a higher band, which would have indicated accumulation of the uncleaved precursor (Fig. 4).

Based on the abnormal appearance of a subset of the mitochondria in CLPP Mut, mitochondrial function was analyzed using Seahorse XFe96 (Agilent Technology). PA-1 cells infected with CLPP Mut demonstrated no difference in the OCR compared with CLPP WT at baseline (44.9 ± 15.0 vs 66.1 ± 21.7 pmol/min; $P = 0.2$) or after carbonyl cyanide P-trifluoromethoxyphenylhydrazone administration, which destroys the mitochondrial membrane potential causing increased flux through the electron transport chain (49.8 ± 16.5 vs 74.5 ± 25.9 pmol/min; $P = 0.2$). Also, no difference was found in OCR after blockade of adenosine triphosphate synthase with oligomycin (26.6 ± 3.7 vs 31.4 ± 10.9 pmol/min; $P = 0.5$) or complex I with rotenone (20.3 ± 2.5 vs 20.3 ± 6.7 pmol/min; $P = 1.0$).

Discussion

We identified deleterious mutations in two previously identified genes causing POI in consanguineous families, *PSMC3IP* and *CLPP*. A mutation in *PSMC3IP* was previously identified in a consanguineous family with primary amenorrhea and POI (30). In addition, recent functional studies have demonstrated that *PSMC3IP* with a C-terminal deletion, similar to that found in our family, fails to associate with the proteins required for homologous recombination (Fig. 5) (33). A male
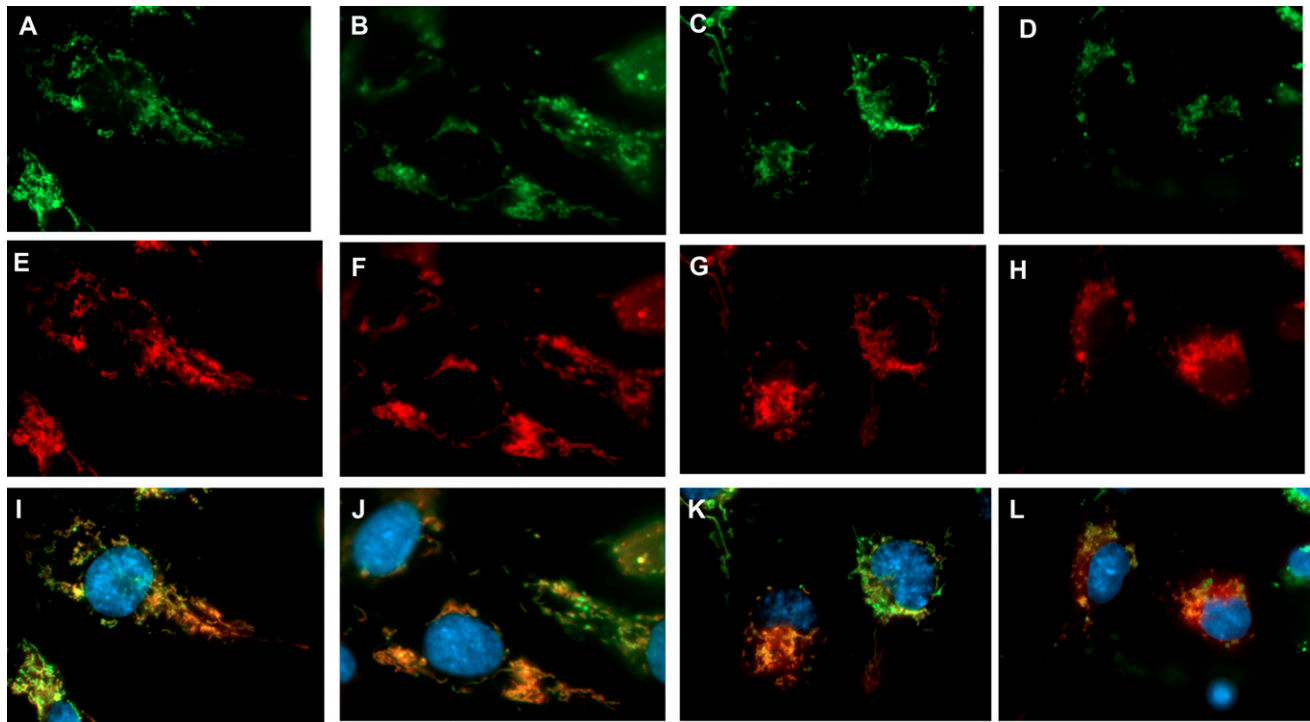
Figure 3. (A) pLenti-CLPP-mGFP with WT CLPP and (B–D) pLenti-CLPP-mGFP with Mut (c.100C>T) CLPP (green) infected cells; (E) WT CLPP-GFP and (F–H) Mut CLPP-GFP infected cells labeled with mitotracker (red) and (I) WT CLPP-GFP and (J–L) Mut CLPP-GFP merged and stained with Hoechst DNA stain (blue). CLPP localized in mitochondria in both CLPP WT and CLPP Mut. CLPP Mut were found with both normal appearing (B, F, J) and fragmented appearing (C, D, G, H, K, L) mitochondria.

homozygote in the family also demonstrated azoospermia, a fertility defect that had not been previously described. Mutations in *CLPP* have been described in consanguineous families with hearing loss and primary amenorrhea from ovarian insufficiency (12, 14). However, although the *CLPP* mutation appeared to cause some mitochondrial fragmentation, no evidence was found for a mitochondrial respiratory defect or processing abnormality. Taken together, strong evidence exists that the homozygous stop gain mutation in *PSMC3IP* is a causal mutation in the family.

The expression pattern and deletion models of *PSMC3IP* in yeast, mice, and humans suggest that both male and female reproductive phenotypes should result from mutations in the gene. In mice, *PSMC3IP* is highly expressed in the testis, specifically in the nucleus of

Figure 4. Western blot demonstrating CLPP-GFP Mut (p.Pro34Ser) and WT localization and size in the mitochondrial fraction. A representative Western blot of the CLPP-GFP and HSP60 protein bands in mitochondria shown.

spermatocytes, which are the forms undergoing meiosis (34). It is less highly expressed in the ovary (34). However, ovarian expression will depend on the presence of oocytes and the stage of oocyte development, which were not specified in their study (34). *PSMC3IP* encodes a protein that is a critical coactivator of DMC1 and RAD51, which are proteins responsible for homologous recombination and double strand break repair in meiosis (30, 33, 35). In yeast and mice, mutation or deletion of the *PSMC3IP* homolog *hop2* results in failure of synaptonemal complex formation. In addition, chromosome synapses form between nonhomologous partners, and single strand tails form but fail to repair after double strand breaks occur (31, 36). The *hop2* mutation then triggers a checkpoint during the pachytene stage, which prevents entry into meiosis I (37). Furthermore, in mouse models in which checkpoint proteins are triggered, the germ cells undergo apoptosis (37).

Mouse deletions in males demonstrate a block at the primary spermatocyte stage, which indicates a block at meiosis I (31). However, the Sertoli cells and spermatogonia are present, as are the Leydig cells. Therefore, testosterone production and pubertal development are normal. Consistent with the presence of the spermatogonia and normal Leydig cell function, the brother in our family had normal puberty with isolated azoospermia caused by the homozygous stop gain *PSMC3IP* mutation.
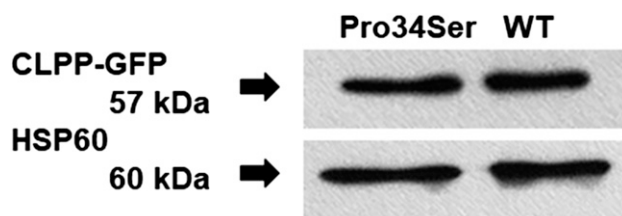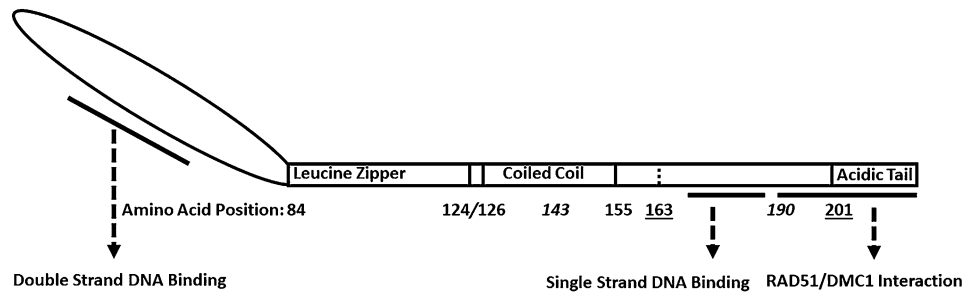
Figure 5. Model of PSMC3IP protein domains and functions, with corresponding human amino acid position noted below. C-terminal deletions modeled previously at amino acid 143 and 190 indicated in italics (33). Deletion at amino acid 143 removes the single strand DNA binding site, and the deletions at 143 and 190 remove the RAD51 and DMC1 interaction sites. The location of the stop gain mutation in the family described at amino acid 163 is underlined and would also remove the single strand DNA and RAD51/DMC1 interaction sites. The previously identified frameshift mutation at amino acid 201 is also underlined and impairs the RAD51 and DMC1 interaction sites (30, 33).

In contrast, when the checkpoint is triggered in female mice, oocytes undergo apoptosis (31), presumably before puberty in our family. Because follicle formation requires the presence of an oocyte, the absence of oocytes results in the absence of follicular granulosa and theca cells and steroidogenesis. Thus, the women in the present family had an absence of pubertal development.

Deletion of the *PSMC3IP* C-terminus from amino acid 143 and beyond abolishes interaction with single strand DNA and RAD51 and DMC1, and deletion from amino acid 190 abolishes interaction with RAD51 and DMC1 (33). The stop gain mutation in the family we have described deletes the C-terminal portion of the protein starting at amino acid 163, which would also abolish interaction with single strand DNA and RAD51 and DMC1 (Fig. 5). An in-frame deletion mutation was previously identified in *PSMC3IP* in a consanguineous family with primary amenorrhea (30). That mutation resulted in the loss of a highly conserved Glu201 in exon 8 of the protein, which was also demonstrated to abolish interaction with RAD51 and DMC1 (30, 33). Therefore, the *PSMC3IP* mutation disrupts homologous recombination and DNA repair, a defect similar to that found in most consanguineous families with nonsyndromic POI described to date (5–7, 9, 10).

In addition to the stop gain mutation in *PSMC3IP*, a homozygous missense mutation was identified in *CLPP*. Homozygous recessive mutations in *CLPP*, a mitochondrial protease, also cause POI and progressive sensorineural hearing loss in males and females (Perrault syndrome) (12–14). The clinical findings in Perrault syndrome conferred by mutations in *CLPP* are broad and heterogeneous, with POI occurring from puberty to the third decade (12, 14). Therefore, the identification of a mutation in *CLPP* in the present family could be hypothesized to support an additional phenotype: POI in the absence of hearing loss.

The homozygous *CLPP* variant in the family described is located in the N-terminal mitochondrial targeting peptide, which is situated before the adenosine triphosphate-dependent Clp protease proteolytic subunit and is important for localization to the mitochondria (32, 38). Therefore, we hypothesized that the variant would disrupt mitochondrial localization. However, mitochondrial localization was normal in amount, as demonstrated by fluorescence microscopy and Western blotting. Nevertheless, some of the mitochondria in the cells infected with Mut CLPP had a fragmented appearance, which was not demonstrated in the WT. After CLPP enters the mitochondria, processing and removal of the targeting peptide by intramitochondrial proteases occurs quickly, within 4 hours of incubation (32). However, the size of the CLPP WT and CLPP Mut was not different, suggesting that the variant does not affect removal of the targeting peptide. Furthermore, no decrease was found in mitochondrial OCR in cells infected with the CLPP Mut. Previous studies in which *CLPP* was completely deleted in mice have demonstrated abnormal mitochondrial morphology but only a minimal mitochondrial respiratory defect (13, 39). Taken together, the data suggest that the missense variant p.Pro34Ser does not result in mitochondrial dysfunction.

In the absence of demonstrable mitochondrial dysfunction, it is unlikely that the *CLPP* variant plays a role in the ovarian insufficiency. Furthermore, the homozygous variant does not appear to affect male fertility, as the father was a homozygote. Finally, the missense variant was homozygous in four subjects in the Saudi Human Genome Program (allele frequency 0.021) and in one subject (allele frequency 0.00015) in the Genome Aggregation Database (gnomAD), the updated ExAC database, which includes whole genome sequences (21), making it less likely to be pathogenic.

In our cohort of 96 subjects with sporadic POI, we did not identify additional mutations in *PSMC3IP*. Also, no mutations were identified in a small Swedish cohort of 50 subjects (40). Although one additional subject with sporadic POI at age 30 years carried a heterozygous

variant in *CLPP* (c.343A>T, p.Ile115Phe), all reported cases were homozygotes. However, it is possible that heterozygous mutations could be responsible for POI presenting at a later age.

In conclusion, the present study has expanded the human phenotype of mutations in *PSMC3IP* from primary amenorrhea and POI to male infertility and azoospermia with normal pubertal development. Our findings also suggest that the N-terminal missense mutation in *CLPP* does not cause substantial mitochondrial dysfunction or contribute to ovarian dysfunction in an oligogenic manner. These data support the increasing body of data demonstrating that homozygous mutations affecting genes involved in homologous recombination and DNA repair cause POI through XX gonadal dysgenesis in females and infertility through isolated azoospermia in males. Thus, including infertile males with normal pubertal development in familial studies of POI might expand the power to detect new mutations.

Acknowledgments

References

1. Welt CK. Primary ovarian insufficiency: a more accurate term for premature ovarian failure. *Clin Endocrinol (Oxf).* 2008;**68**(4): 499–509.

2. Torgerson DJ, Thomas RE, Reid DM. Mothers and daughters menopausal ages: is there a link? *Eur J Obstet Gynecol Reprod Biol.* 1997;**74**(1):63–66.

3. de Bruin JP, Bovenhuis H, van Noord PA, Pearson PL, van Arendonk JA, te Velde ER, Kuurman WW, Dorland M. The role of genetic factors in age at natural menopause. *Hum Reprod.* 2001; **16**(9):2014–2018.

4. Snieder H, MacGregor AJ, Spector TD. Genes control the cessation of a woman's reproductive life: a twin study of hysterectomy and age at menopause. *J Clin Endocrinol Metab.* 1998;**83**(6):1875–1880.

5. de Vries L, Behar DM, Smirin-Yosef P, Lagovsky I, Tzur S, Basel-Vanagaite L. Exome sequencing reveals SYCE1 mutation associated with autosomal recessive primary ovarian insufficiency. *J Clin Endocrinol Metab.* 2014;**99**(10):E2129–E2132.

6. Caburet S, Arboleda VA, Llano E, Overbeek PA, Barbero JL, Oka K, Harrison W, Vaiman D, Ben-Neriah Z, García-Tuñón I, Fellous M, Pendás AM, Veitia RA, Vilain E. Mutant cohesin in premature ovarian failure. *N Engl J Med.* 2014;**370**(10):943–949.

7. Wood-Trageser MA, Gurbuz F, Yatsenko SA, Jeffries EP, Kotan LD, Surti U, Ketterer DM, Matic J, Chipkin J, Jiang H, Trakselis MA, Topaloglu AK, Rajkovic A. MCM9 mutations are associated with ovarian failure, short stature, and chromosomal instability. *Am J Hum Genet.* 2014;**95**(6):754–762.

8. Katari S, Wood-Trageser MA, Jiang H, Kalynchuk E, Muzumdar R, Yatsenko SA, Rajkovic A. Novel inactivating mutation of the FSH receptor in two siblings of Indian origin with premature ovarian failure. *J Clin Endocrinol Metab.* 2015;**100**(6):2154–2157.

9. AlAsiri S, Basit S, Wood-Trageser MA, Yatsenko SA, Jeffries EP, Surti U, Ketterer DM, Afzal S, Ramzan K, Faiyaz-Ul Haque M, Jiang H, Trakselis MA, Rajkovic A. Exome sequencing reveals MCM8 mutation underlies ovarian failure and chromosomal instability. *J Clin Invest.* 2015;**125**(1):258–262.

10. Smirin-Yosef P, Zuckerman-Levin N, Tzur S, Granot Y, Cohen L, Sachsenweger J, Borck G, Lagovsky I, Salmon-Divon M, Wiesmüller L, Basel-Vanagaite L. A biallelic mutation in the homologous recombination repair gene SPIDR is associated with human gonadal dysgenesis. *J Clin Endocrinol Metab.* 2017;**102**(2):681–688.

11. Fogli A, Rodriguez D, Eymard-Pierre E, Bouhour F, Labauge P, Meaney BF, Zeesman S, Kaneski CR, Schiffmann R, Boespflug-Tanguy O. Ovarian failure related to eukaryotic initiation factor 2B mutations. *Am J Hum Genet.* 2003;**72**(6):1544–1550.

12. Jenkinson EM, Rehman AU, Walsh T, Clayton-Smith J, Lee K, Morell RJ, Drummond MC, Khan SN, Naeem MA, Rauf B, Billington N, Schultz JM, Urquhart JE, Lee MK, Berry A, Hanley NA, Mehta S, Cilliers D, Clayton PE, Kingston H, Smith MJ, Warner TT, Black GC, Trump D, Davis JR, Ahmad W, Leal SM, Riazuddin S, King MC, Friedman TB, Newman WG; University of Washington Center for Mendelian Genomics. Perrault syndrome is caused by recessive mutations in CLPP, encoding a mitochondrial ATP-dependent chambered protease. *Am J Hum Genet.* 2013;**92**(4):605–613.

13. Gispert S, Parganlija D, Klinkenberg M, Dröse S, Wittig I, Mittelbronn M, Grzmil P, Koob S, Hamann A, Walter M, Büchel F, Adler T, Hrabé de Angelis M, Busch DH, Zell A, Reichert AS, Brandt U, Osiewacz HD, Jendrach M, Auburger G. Loss of mitochondrial peptidase Clpp leads to infertility, hearing loss plus growth retardation via accumulation of CLPX, mtDNA and inflammatory factors. *Hum Mol Genet.* 2013;**22**(24):4871–4887.

14. Ahmed S, Jelani M, Alrayes N, Mohamoud HS, Almramhi MM, Anshasi W, Ahmed NA, Wang J, Nasir J, Al-Aama JY. Exome analysis identified a novel missense mutation in the CLPP gene in a consanguineous Saudi family expanding the clinical spectrum of Perrault Syndrome type-3. *J Neurol Sci.* 2015;**353**(1-2):149–154.

15. Lourenço D, Brauner R, Lin L, De Perdigo A, Weryha G, Muresan M, Boudjenah R, Guerra-Junior G, Maciel-Guerra AT, Achermann JC, McElreavey K, Bashamboo A. Mutations in NR5A1 associated with ovarian insufficiency. *N Engl J Med.* 2009;**360**(12): 1200–1210.

16. Maor-Sagie E, Cinnamon Y, Yaacov B, Shaag A, Goldsmidt H, Zenvirt S, Laufer N, Richler C, Frumkin A. Deleterious mutation in SYCE1 is associated with non-obstructive azoospermia. *J Assist Reprod Genet.* 2015;**32**(6):887–891.

17. Tenenbaum-Rakover Y, Weinberg-Shukron A, Renbaum P, Lobel O, Eideh H, Gulsuner S, Dahary D, Abu-Rayyan A, Kanaan M, Levy-Lahad E, Bercovich D, Zangen D. Minichromosome

maintenance complex component 8 (MCM8) gene mutations result in primary gonadal failure. *J Med Genet*. 2015;**52**(6):391–399.

18. The 1000 Genomes Project Consortium, Abecasis GR, Auton A, Brooks LD, DePristo MA, Durbin RM, Handsaker RE, Kang HM, Marth GT, McVean GA. An integrated map of genetic variation from 1,092 human genomes. *Nature*. 2012;**491**(7422):56–65.

19. Hu H, Roach JC, Coon H, Guthery SL, Voelkerding KV, Margraf RL, Durtschi JD, Tavtigian SV, Shankaracharya, Wu W, Scheet P, Wang S, Xing J, Glusman G, Hubley R, Li H, Garg V, Moore B, Hood L, Galas DJ, Srivastava D, Reese MG, Jorde LB, Yandell M, Huff CD. A unified test of linkage analysis and rare-variant association for analysis of pedigree sequence data. *Nat Biotechnol*. 2014;**32**(7):663–669.

20. Kennedy B, Kronenberg Z, Hu H, Moore B, Flygare S, Reese MG, Jorde LB, Yandell M, Huff C. Using VAAST to identify disease-associated variants in next-generation sequencing data. *Curr Protoc Hum Genet*. 2014;**81**:6.14.1–6.14.25.

21. Lek M, Karczewski KJ, Minikel EV, Samocha KE, Banks E, Fennell T, O'Donnell-Luria AH, Ware JS, Hill AJ, Cummings BB, Tukiainen T, Birnbaum DP, Kosmicki JA, Duncan LE, Estrada K, Zhao F, Zou J, Pierce-Hoffman E, Berghout J, Cooper DN, Deflaux N, DePristo M, Do R, Flannick J, Fromer M, Gauthier L, Goldstein J, Gupta N, Howrigan D, Kiezun A, Kurki MI, Moonshine AL, Natarajan P, Orozco L, Peloso GM, Poplin R, Rivas MA, Ruano-Rubio V, Rose SA, Ruderfer DM, Shakir K, Stenson PD, Stevens C, Thomas BP, Tiao G, Tusie-Luna MT, Weisburd B, Won HH, Yu D, Altshuler DM, Ardissino D, Boehnke M, Danesh J, Donnelly S, Elosua R, Florez JC, Gabriel SB, Getz G, Glatt SJ, Hultman CM, Kathiresan S, Laakso M, McCarroll S, McCarthy MI, McGovern D, McPherson R, Neale BM, Palotie A, Purcell SM, Saleheen D, Scharf JM, Sklar P, Sullivan PF, Tuomilehto J, Tsuang MT, Watkins HC, Wilson JG, Daly MJ, MacArthur DG, Exome Aggregation C; Exome Aggregation Consortium. Analysis of protein-coding genetic variation in 60,706 humans. *Nature*. 2016; **536**(7616):285–291.

22. NHLBI GO Exome Sequencing Project (ESP). Available at: http://evs.gs.washington.edu/EVS/. Accessed October 2017.

23. Coonrod EM, Margraf RL, Russell A, Voelkerding KV, Reese MG. Clinical analysis of genome next-generation sequencing data using the Omicia platform. *Expert Rev Mol Diagn*. 2013;**13**(6):529–540.

24. Yandell M, Huff C, Hu H, Singleton M, Moore B, Xing J, Jorde LB, Reese MG. A probabilistic disease-gene finder for personal genomes. *Genome Res*. 2011;**21**(9):1529–1542.

25. Pollard KS, Hubisz MJ, Rosenbloom KR, Siepel A. Detection of nonneutral substitution rates on mammalian phylogenies. *Genome Res*. 2010;**20**(1):110–121.

26. Singleton MV, Guthery SL, Voelkerding KV, Chen K, Kennedy B, Margraf RL, Durtschi J, Eilbeck K, Reese MG, Jorde LB, Huff CD, Yandell M. Phevor combines multiple biomedical ontologies for accurate identification of disease-causing alleles in single individuals and small nuclear families. *Am J Hum Genet*. 2014;**94**(4): 599–610.

27. Köhler S, Vasilevsky NA, Engelstad M, Foster E, McMurry J, Aymé S, Baynam G, Bello SM, Boerkoel CF, Boycott KM, Brudno M, Buske OJ, Chinnery PF, Cipriani V, Connell LE, Dawkins HJ, DeMare LE, Devereau AD, de Vries BB, Firth HV, Freson K, Greene D, Hamosh A, Helbig I, Hum C, Jähn JA, James R, Krause R, F Laulederkind SJ, Lochmüller H, Lyon GJ, Ogishima S, Olry A,

Ouwehand WH, Pontikos N, Rath A, Schaefer F, Scott RH, Segal M, Sergouniotis PI, Sever R, Smith CL, Straub V, Thompson R, Turner C, Turro E, Veltman MW, Vulliamy T, Yu J, von Ziegenweidt J, Zankl A, Züchner S, Zemojtel T, Jacobsen JO, Groza T, Smedley D, Mungall CJ, Haendel M, Robinson PN. The human phenotype ontology in 2017. *Nucleic Acids Res*. 2017; **45**(D1):D865–D876.

28. Moriwaki M, Moore B, Mosbruger T, Neklason DW, Yandell M, Jorde LB, Welt CK. POLR2C mutations are associated with primary ovarian insufficiency in women. *J Endocr Soc*. 2017;**1**(3): 162–173.

29. Schell JC, Olson KA, Jiang L, Hawkins AJ, Van Vranken JG, Xie J, Egnatchik RA, Earl EG, DeBerardinis RJ, Rutter J. A role for the mitochondrial pyruvate carrier as a repressor of the Warburg effect and colon cancer cell growth. *Mol Cell*. 2014;**56**(3):400–413.

30. Zangen D, Kaufman Y, Zeligson S, Perlberg S, Fridman H, Kanaan M, Abdulhadi-Atwan M, Abu Libdeh A, Gussow A, Kisslov I, Carmel L, Renbaum P, Levy-Lahad E. XX ovarian dysgenesis is caused by a PSMC3IP/HOP2 mutation that abolishes coactivation of estrogen-driven transcription. *Am J Hum Genet*. 2011;**89**(4): 572–579.

31. Petukhova GV, Romanienko PJ, Camerini-Otero RD. The Hop2 protein has a direct role in promoting interhomolog interactions during mouse meiosis. *Dev Cell*. 2003;**5**(6):927–936.

32. Corydon TJ, Bross P, Holst HU, Neve S, Kristiansen K, Gregersen N, Bolund L. A human homologue of *Escherichia coli* ClpP caseinolytic protease: recombinant expression, intracellular processing and subcellular localization. *Biochem J*. 1998;**331**(Pt 1): 309–316.

33. Zhao W, Sung P. Significance of ligand interactions involving Hop2-Mnd1 and the RAD51 and DMC1 recombinases in homologous DNA repair and XX ovarian dysgenesis. *Nucleic Acids Res*. 2015;**43**(8):4055–4066.

34. Ko L, Cardona GR, Henrion-Caude A, Chin WW. Identification and characterization of a tissue-specific coactivator, GT198, that interacts with the DNA-binding domains of nuclear receptors. *Mol Cell Biol*. 2002;**22**(1):357–369.

35. Sansam CL, Pezza RJ. Connecting by breaking and repairing: mechanisms of DNA strand exchange in meiotic recombination. *FEBS J*. 2015;**282**(13):2444–2457.

36. Leu JY, Chua PR, Roeder GS. The meiosis-specific Hop2 protein of S. cerevisiae ensures synapsis between homologous chromosomes. *Cell*. 1998;**94**(3):375–386.

37. Roeder GS, Bailis JM. The pachytene checkpoint. *Trends Genet*. 2000;**16**(9):395–403.

38. de Sagarra MR, Mayo I, Marco S, Rodríguez-Vilariño S, Oliva J, Carrascosa JL, Casta ñ JG. Mitochondrial localization and oligomeric structure of HClpP, the human homologue of *E. coli* ClpP. *J Mol Biol*. 1999;**292**(4):819–825.

39. Szczepanowska K, Maiti P, Kukat A, Hofsetz E, Nolte H, Senft K, Becker C, Ruzzenente B, Hornig-Do HT, Wibom R, Wiesner RJ, Krüger M, Trifunovic A. CLPP coordinates mitoribosomal assembly through the regulation of ERAL1 levels. *EMBO J*. 2016; **35**(23):2566–2583.

40. Norling A, Hirschberg AL, Karlsson L, Rodriguez-Wallberg KA, Iwarsson E, Wedell A, Barbaro M. No mutations in the PSMC3IP gene identified in a Swedish cohort of women with primary ovarian insufficiency. *Sex Dev*. 2014;**8**(4):146–150.